

QC851  
.C47  
no. 31  
ATMOS

ISSN No. 0737-5352-31

SIZE CORRECTIONS BASED ON REFRACTIVE INDEX  
FOR PARTICLE MEASURING SYSTEMS  
ACTIVE SCATTERING AEROSOL SPECTROMETER PROBE  
(ASASP-X)

Jennifer L. Hand and Sonia M. Kreidenweis

Department of Atmospheric Science  
Colorado State University  
Fort Collins, CO

Funding Agency:  
National Park Service # 1443-CA0001-92-006 96.5

January, 1996

**CIRA** Cooperative Institute for Research in the Atmosphere

---

LIBRARIES  
AUG 03 1999  
COLORADO STATE UNIVERSITY

Colorado  
State  
University

**SIZE CORRECTIONS BASED ON REFRACTIVE INDEX  
FOR PARTICLE MEASURING SYSTEMS  
ACTIVE SCATTERING AEROSOL SPECTROMETER PROBE  
(ASASP-X)**

Jennifer L. Hand and Sonia M. Kreidenweis

Department of Atmospheric Science  
Colorado State University  
Fort Collins, CO

Funding Agency:  
National Park Service # 1443-CA0001-92-006 96.5

January, 1996



U18401 6781787

QC  
851  
.C47  
no. 31  
ATMDS

**SIZE CORRECTIONS BASED ON REFRACTIVE INDEX  
FOR PARTICLE MEASURING SYSTEMS  
ACTIVE SCATTERING AEROSOL SPECTROMETER PROBE  
(ASASP-X)**

Jennifer L. Hand  
Sonia M. Kreidenweis

Department of Atmospheric Science  
Colorado State University  
Fort Collins, CO

COLORADO STATE UNIVERSITY LIBRARIES

## **Abstract**

The response function for the ASASP-X is affected by the optical properties of atmospheric aerosols. The manufacturer calibration is based on polystyrene latex spheres ( $m=1.588-0i$ ), therefore the size distributions derived from measurements taken with the ASASP-X should be corrected for particles of different refractive index. Corrections based on the manufacturer calibration and Mie theory are used to derive size corrections for different refractive indices. These corrections are applied to data and demonstrate the significant over and underestimation of aerosol volume distributions possible if no corrections to diameter are applied.

## **Introduction**

Optical methods are frequently used for the counting and sizing of aerosol particles in the 0.1-10  $\mu\text{m}$  diameter range, where other techniques, such as measurement of electrical mobility, are not as effective. An optical probe was used for the measurement of atmospheric aerosol size distributions in the SEAVS (South Eastern Aerosol and Visibility Study) field project, conducted in the summer of 1995 in the Great Smoky Mountains National Park. As part of this study, the ambient aerosol was conditioned prior to measurement by exposing it to controlled relative humidity, which was varied from very dry to above 90%. It was desired to use the shift in the measured wet and dry aerosol size distributions to determine the aerosol water content. However, this calculation is quite sensitive to uncertainty and errors in the measured optical particle sizes, thus motivating the calibration study presented here.

The standardized calibration used for the Particle Measuring Systems ASASP-X is for polystyrene latex particles (PSL) and neglects to take into account differences in instrument response that arise from different optical properties for atmospheric particles. Previous workers have shown that the response of the probe changes depending on refractive index of the particles (Garvey and Pinnick, 1983; Kim and Boatman, 1990; Hering and McMurry, 1991). These changes in the response can have a large effect on the size distributions measured from the probes, especially when the standardized size bins are used without any corrections to the response (Kim and Boatman, 1990).

The ASASP-X has four overlapping size ranges, each range divided into 15 size bins, with an overall range of 0.09  $\mu\text{m}$  to 3.00  $\mu\text{m}$ . The method by which the particles are sized is the following. The light that is scattered when the particle passes through the He-

Ne laser ( $\lambda=632.8$  nm) is collected by the optics in the probe and focused to a single photodiode which converts the scattered light into a signal. Depending on the strength of the signal, the particle gets sized by the probe into a size bin. This sizing depends completely on the manufacturer calibration, which determines the correspondence between voltage and size bin.

## I. Manufacturer Calibration

Given in the ASASP manual are four diagrams showing the relationship between voltage and size bin for the four ranges. The curve for range 1 is reproduced here as Figure 1.

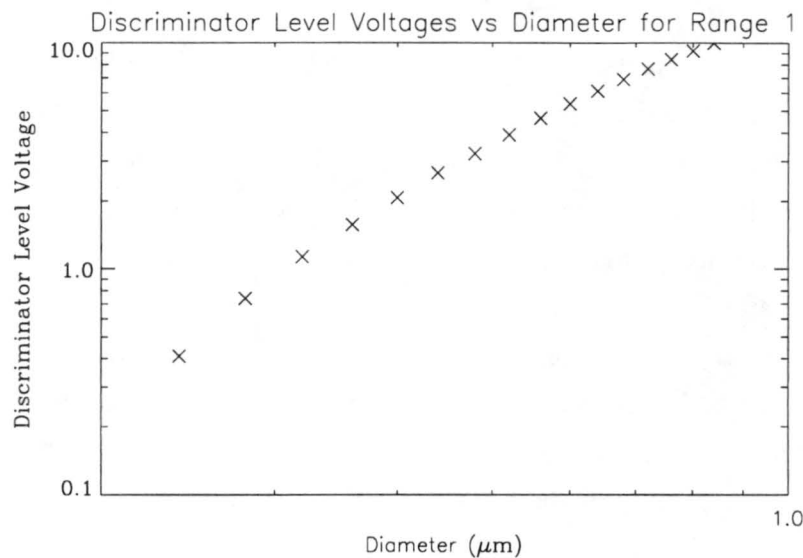


**Figure 1.** Discriminator level voltages from the PMS manual for range 1.

Each range is normalized to 10 volts, so that for each range, the discriminator level voltages vary from 0 to 10 volts. These values can be measured and for our probe, measurements agreed well with values provided in the PMS manual. Programmable amplifiers in the electronics are used to amplify the signals from the smaller size ranges, with 10 V corresponding to the uppermost channel limit of range 0 (largest diameter range). One can determine the manufacturer calibration by dividing the discriminator level voltages by the relative gain ratios (relative to range 0) for each range. These voltage levels are then related to particle size based on Mie scattering theory, which will be described in more detail in the following sections.

The manufacturer verification of the voltage-to-size relationship used by the instrument was performed using latex spheres of known size (PMS Manual, 1977). The voltage response of these spheres is plotted on the calibration curves of voltage verses size bin, and for all of the tested spheres agrees well with the curves, i.e. the spheres are sized in the correct bins. What is not taken into account during this calibration is the effect of index of refraction on the scattering response. Because the smoothed calibration corresponds to polystyrene latex spheres ( $m=1.588-0i$ ), the relationship between voltages and particle sizes assumes that the instrument is insensitive to the optical properties of other particles (PMS Manual, 1977). In this work the correct scattering response functions for particles of other indices of refraction will be determined using Mie scattering theory, as well as methods developed to correct the size bins used by the ASASP-X.

## II. Mie Theoretical Response Functions

Following the methods of Garvey and Pinnick (1983), as well as Kim and Boatman (1990), the theoretical ASASP-X scattering responses ( $\text{cm}^2/\text{particle}$ ) were reproduced for different indices of refraction using the following equation:

$$R = \frac{\pi}{k^2} \int_{\alpha}^{\beta} [ |S_1(\theta) + S_1(\pi - \theta)|^2 + |S_2(\theta) + S_2(\pi - \theta)|^2 ] \sin \theta \, d\theta$$

where  $S_1(x, m, \theta)$  and  $S_2(x, m, \theta)$  are the Mie scattering functions corresponding to light with its electric vector polarized perpendicular and parallel to the scattering plane, respectively. They depend on the index of refraction,  $m$ , the particle size parameter,  $x=kr$  ( $k$  is the wavenumber), and the scattering angle  $\theta$ . The integration is from  $\alpha=35^\circ$  to  $\beta=120^\circ$  for the ASASP-X.  $S_1(x, m, \theta)$  and  $S_2(x, m, \theta)$  were calculated using the BHMIE code given in Bohren and Huffman (1983).

The rural aerosol model provided by Kim and Boatman (1990), composed of a mixture of 70% water soluble particles (ammonia, calcium sulfate, and organic compounds) and 30% dustlike particles, was used here because this model approaches the expected composition of particles measured with the ASASP-X in the Great Smoky Mountains. Kim and Boatman (1990) provide indices of refraction corresponding to various relative humidities (RH) since aerosol water content and hence refractive index change substantially with RH; these are reproduced in Table 1. The theoretical response

for these different indices of refraction can be seen in Figure 2. From this figure it is obvious that the Mie response changes noticeably with refractive index.

**Table 1.** Relative humidities and corresponding refractive indices using the Rural aerosol model.

<b>Relative Humidity</b>	<b>Rural Aerosol Refractive Index</b>
0%	$1.530-6.60 \times 10^{-3}i$
50%	$1.520-6.26 \times 10^{-3}i$
70%	$1.501-5.60 \times 10^{-3}i$
80%	$1.443-3.70 \times 10^{-3}i$
90%	$1.399-2.22 \times 10^{-3}i$
99%	$1.359-9.16 \times 10^{-4}i$

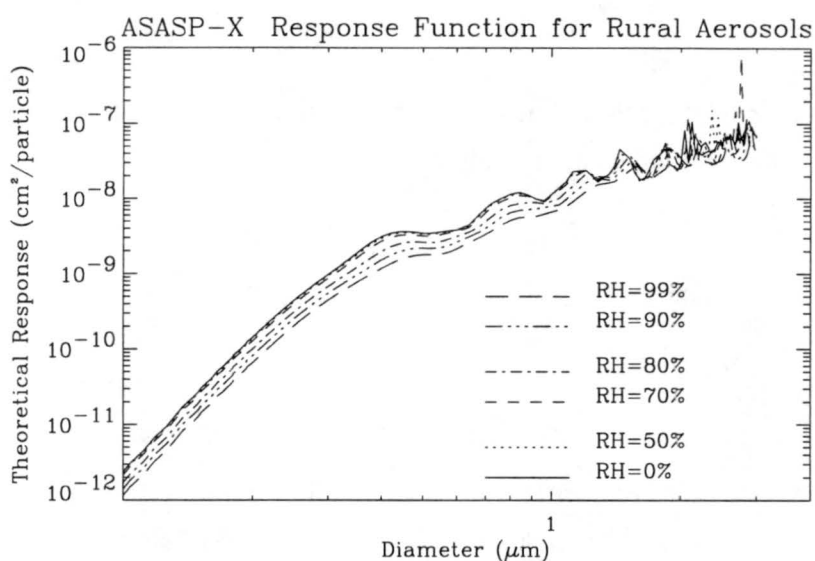


**Figure 2.** Mie theoretical response functions corresponding to the relative humidities in Table 1.

The general approach used here is as follows. The original instrument calibration assigns diameter values to voltage readings, as shown in Figure 1. The voltage and the scattering cross section (the theoretical response,  $\text{cm}^2/\text{particle}$ , shown on the ordinate in Figure 2) have been determined for PSL, as described more fully in Section VI. The normalization constant applied here was determined for the ASASP-X by Garvey and Pinnick (1983) ( $C=1.9 \times 10^8 \text{ V cm}^{-2}$ ) and also applied are their reported relative gains for each range. Measured voltages can then be converted to a scattering cross section (TR) using the following equation:  $\text{TR} = \text{DLV}/(C \times \text{RG})$  where DLV is the discriminator level

voltage,  $C$  is the normalization constant, and  $RG$  is the relative gain. Table 2 presents the resulting relationship between channel voltage limits, cross section (assuming  $C=1.9 \times 10^8$   $V\text{ cm}^{-2}$ ), and corresponding PSL diameters as suggested by the manufacturer (hereafter called PMS diameter).

**Table 2.** ASASP-X channel limits, voltages, and diameters for four ranges from the PMS manual. Cross sections were determined using a normalization constant of  $C=1.9 \times 10^8$   $V\text{ cm}^{-2}$  and relative gains used were those provided in Garvey and Pinnick (1983).

channel	Range 0			Range 1			Range 2			Range 3		
	volts	cross-section ( $\text{cm}^2$ )	Dp ( $\mu\text{m}$ )	volts	cross-section ( $\text{cm}^2$ )	Dp ( $\mu\text{m}$ )	volts	cross-section ( $\text{cm}^2$ )	Dp ( $\mu\text{m}$ )	volts	cross-section ( $\text{cm}^2$ )	Dp ( $\mu\text{m}$ )
	0.604	3.179e-09	0.6	0.0648	3.411e-10	0.24	0.0056	2.947e-11	0.15	0.000327	1.721e-12	0.090
1	1.42	7.474e-09	0.76	0.117	6.158e-10	0.28	0.00797	4.195e-11	0.16	0.00053	2.789e-12	0.097
2	2.11	1.111e-08	0.92	0.179	9.421e-10	0.32	0.0111	5.842e-11	0.17	0.000771	4.058e-12	0.104
3	2.75	1.447e-08	1.08	0.249	1.311e-09	0.36	0.0152	8.000e-11	0.18	0.00111	5.842e-12	0.111
4	3.39	1.784e-08	1.24	0.329	1.732e-09	0.40	0.0205	1.079e-10	0.19	0.00158	8.316e-12	0.118
5	4.04	2.126e-08	1.40	0.423	2.226e-09	0.44	0.027	1.421e-10	0.20	0.00217	1.142e-11	0.125
6	4.68	2.463e-08	1.56	0.513	2.700e-09	0.48	0.0348	1.832e-10	0.21	0.00293	1.542e-11	0.132
7	5.3	2.789e-08	1.72	0.621	3.268e-09	0.52	0.0441	2.321e-10	0.22	0.00386	2.032e-11	0.139
8	5.92	3.116e-08	1.88	0.734	3.863e-09	0.56	0.0542	2.853e-10	0.23	0.00499	2.626e-11	0.146
9	6.54	3.442e-08	2.04	0.85	4.474e-09	0.60	0.0653	3.437e-10	0.24	0.00635	3.342e-11	0.153
10	7.16	3.768e-08	2.20	0.967	5.089e-09	0.64	0.0771	4.058e-10	0.25	0.0080	4.211e-11	0.160
11	7.76	4.084e-08	2.36	1.09	5.737e-09	0.68	0.0897	4.721e-10	0.26	0.0100	5.263e-11	0.167
12	8.35	4.395e-08	2.52	1.22	6.421e-09	0.72	0.103	5.421e-10	0.27	0.0123	6.474e-11	0.174
13	8.92	4.695e-08	2.68	1.34	7.053e-09	0.76	0.117	6.158e-10	0.28	0.0151	7.947e-11	0.181
14	9.47	4.984e-08	2.84	1.46	7.684e-09	0.80	0.132	6.947e-10	0.29	0.0185	9.737e-11	0.188
15	10.0	5.263e-08	3.00	1.58	8.316e-09	0.84	0.147	7.737e-10	0.30	0.0227	1.195e-10	0.195

In this work, a new relationship between voltage, equivalent to scattering cross section, and particle diameter is sought that is appropriate for a different refractive index. In Figure 2, this is equivalent to finding the relationship between the PSL diameter having a selected cross section and the ambient particle diameter, at a certain RH, having the same cross section.

An obvious problem in determining sizes from the Mie theoretical response is that the Mie resonances result in multiple values of diameter for a given voltage or response. One solution to this problem would be to ‘lump’ size bins corresponding to multivalued theoretical response (for example, see the .4  $\mu\text{m}$ -.6  $\mu\text{m}$  range for  $RH=0\%$ ). This lumping would result in lost sensitivity, but because the instrument resolution in this region is artificial, the loss of sensitivity is of no great consequence. By examining Figure 2, it is

seen that the multivalued range occurs in different regions for different indices of refraction, therefore one would expect each curve to have lumped channels in different regions. The ultimate goal is to derive new size bins for each index of refraction, while taking into account these multivalued regions. There appear to be several approaches to this problem.

### III. Fitting by Linear Regression

The first method tested was the linear regression technique described by Kim and Boatman (1990) and applied by them to the recalibration of the ASASP-100X, a 15 channel probe spanning the diameter range of 0.12-3.12  $\mu\text{m}$ . Kim and Boatman fit linear regressions through the scattering cross sections for the new refractive index. Piece-wise fitting was performed through adjacent size channels, and the probe diameters were corrected for refractive index. Figure 3 shows the ratio of probe diameter to corrected diameter for RH=90%. The corrected diameters found by Kim and Boatman are larger than the manufacturer calibration diameters for the entire range.

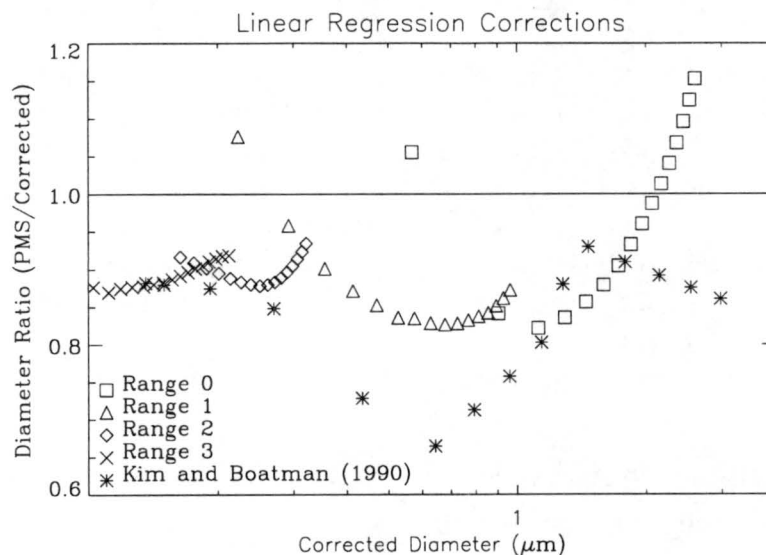


**Figure 3.** Ratio of PMS diameter to corrected diameter for Kim and Boatman (1990), as well as corrections made by linear regression fits for the ASASP-X for all ranges. Corrections were made for a relative humidity of 90%.

This approach was adapted for the ASASP-X by determining the cross sections corresponding to the manufacturer voltage calibration for each range (described further in Section IV). The values spanning the upper and lower limits of cross section corresponding to the manufacturer calibration range were used to fit a line through the relevant portion of the theoretical Mie response curve for a specific RH. For each cross

section corresponding to the manufacturer calibration channel limit, a corrected diameter was derived from the equation of the line. This method was repeated for each of the four ranges. The resulting linear fits can be found in Figure 4 along with the manufacturer calibration and the Mie theoretical response for RH=90%.

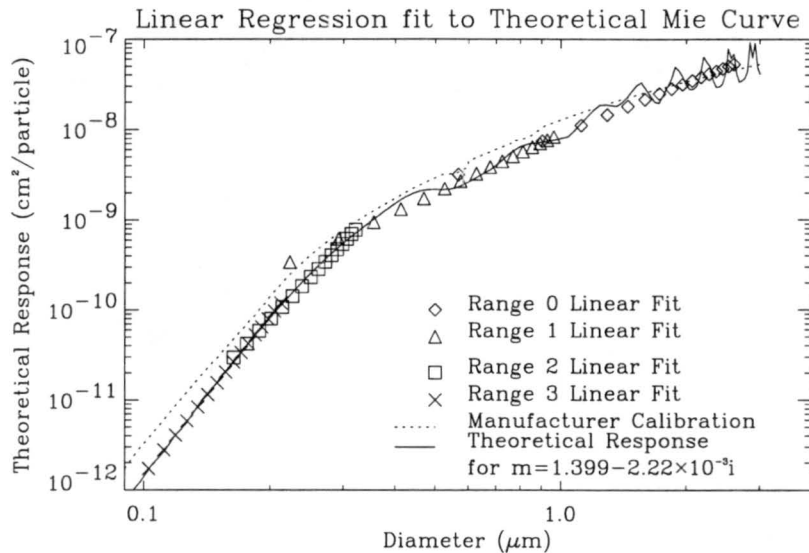


**Figure 4.** Linear fits for each of the four ranges, plotted with the Mie theoretical response for  $m=1.399-2.22 \times 10^{-3}i$ . The manufacturer calibration is plotted for comparison.

Figure 3 shows the ratio of PMS to corrected diameter for all four ranges. The corrected diameters are smaller than those determined by Kim and Boatman (1990) and, in Range 0, the corrected diameters are smaller than the manufacturer's calibration. Ratios  $>1$  in Range 0 occur because of the curvature of the manufacturer calibration (see Figure 4). At large diameter ( $>1 \mu\text{m}$ ), cross section values are smaller for the manufacturer calibration than for the theoretical response for RH=90%, resulting in undersizing. The manufacturer calibration for the ASASP-100X used by Kim and Boatman (1990) may have a different curvature, resulting in consistently larger and corrected diameters (seen in Figure 3).

Discrepancies exist in the regions of overlapping diameters between ranges which are due to the discontinuities in the linear fits between ranges (Figure 4). Smoothing through the entire Mie curve would be advantageous in avoiding difficulties associated with overlapping regions of the linear fits, and in fact this method is discussed and applied in the following section. The linear regression method smooths through the flat regions of the Mie curve which produces artificial resolution. Any piece-wise or smooth fit through the Mie curve for different refractive index will result in artificial resolution in the multivalued

regions. A method resulting in automatic lumping of these regions will be discussed in Section VI.

#### IV. Fitting by Polynomial to Polynomial

The next attempt in determining corrected size ranges incorporates the manufacturer calibration and smoothed responses for other refractive indices. Figure 5 shows the PSL Mie curve plotted against the manufacturer calibration from Table 2.

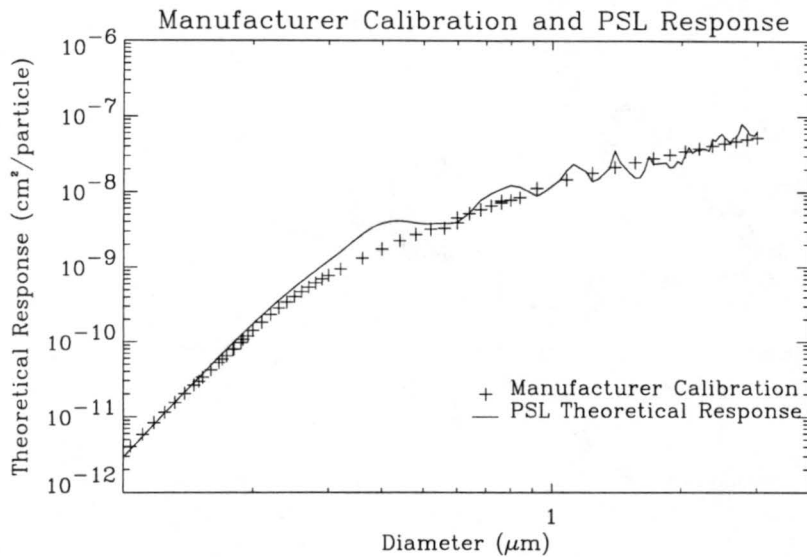


**Figure 5.** PSL theoretical Mie response plotted with the manufacturer calibration. In certain regions, the calibration is not a representative fit through the Mie curve.

The smoothing of the true response which has been assumed is evident. It is also seen that in some regions, the calibration is not very representative of the Mie scattering curve. The dependence of this fit on the gains and the normalization constant is obvious.

Smooth fits of the curves for other values of refractive index were determined by fitting them with cubic polynomials; the results for one refractive index corresponding to RH=90% are shown in Figure 6.

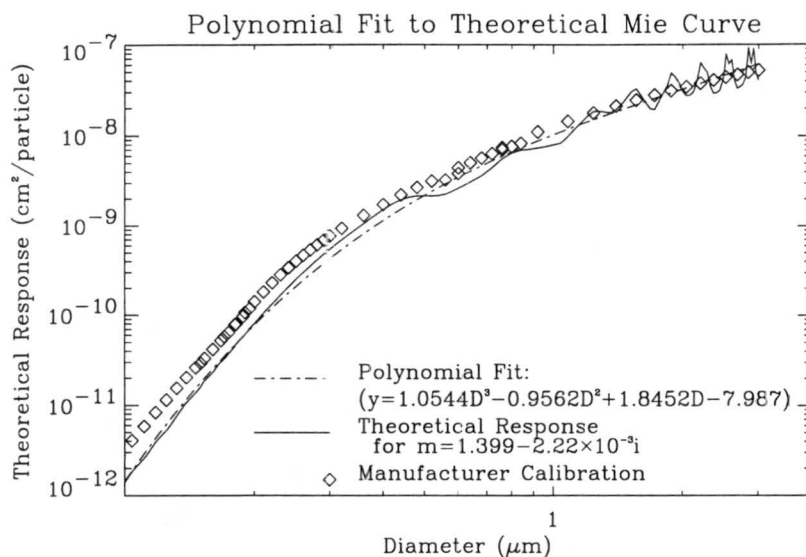


**Figure 6.** Polynomial fit through the theoretical response for  $m=1.399-2.22\times 10^{-3}i$ . The manufacturer calibration is plotted for comparison.

Noticeably, the smoothing through the resonances results in no multivalued response problem. Using these curves, corrected size bins were determined in the following way. The manufacturer calibration was fit to a polynomial with a correlation of 1. The resulting equation of the polynomial was used to determine the theoretical response for the corresponding PMS diameters. Theoretical responses were set equal to the polynomial equation for the desired refractive index and solved for the corresponding diameter. Figure 7 shows the ratio of PMS diameter to corrected diameter.

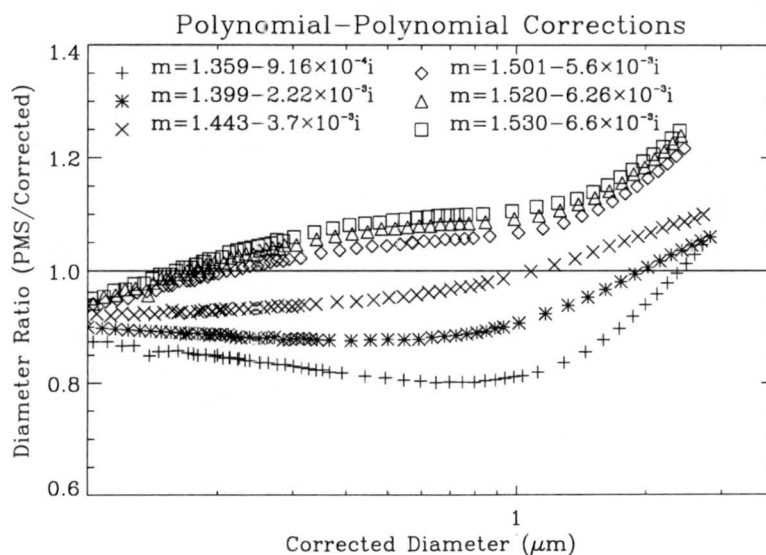


**Figure 7.** Ratio of PMS to corrected diameter for polynomial-polynomial corrections as a function of corrected diameter, for the refractive indices found in Table 1.

For refractive indices similar to that of PSL ( $1.53 > \Re(m) > 1.443$ ), the diameter corrections are within 10% of the manufacturer calibration for particle sizes under  $1 \mu\text{m}$ . Interestingly, corrections are obtained even for refractive indices very close to PSL ( $\Re(m)=1.588$ ). This occurs because the polynomial fits derived here have different curvature than the manufacturer calibration, often fitting the shape of the Mie curve better. In particular, substantial differences are found for  $D_p > 1 \mu\text{m}$ , which result from different smoothing through the Mie resonances at larger particle size.

For refractive indices substantially different from PSL ( $\Re(m) < 1.443$ ), significant corrections are obtained over the entire size range. The true diameter is always larger than that assigned by the probe, except for the largest few size channels. From this method, it is obvious that any changes in the manufacturer voltage calibration, or in the normalization constant, will have a large effect on the results.

## V. Mie Curve to Mie Curve Corrections

The work presented in this section was motivated by the work of Hering and McMurry (1991). They determined diameter corrections for ambient aerosol versus PSL that were larger than those determined here using the previous method. Using the PMS LAS-X optical counter (16 size channels in the  $0.09\text{-}3 \mu\text{m}$  size range), a differential mobility analyzer (DMA), and a pulse height analyzer, Hering and McMurry (1991) measured the peak height voltages and sizes of PSL, oleic acid, and atmospheric aerosols. Any dependence on the manufacturer voltage-diameter calibration was circumvented by measuring the peak height voltages and using the DMA to determine geometric particle size. However, a normalization constant used to convert voltages to cross section was determined by fitting theoretical calculations to the PSL voltage response at one diameter ( $0.5 \mu\text{m}$ ) and applying this same constant to oleic acid measurements. Diameter corrections were determined for atmospheric aerosols. In the diameter range of  $0.1\text{-}1 \mu\text{m}$ , the diameters determined by the optical counter, which were based on the measured PSL response as described above, were often significantly smaller than the actual diameters. Their results are reproduced here as Figure 8a. It is also seen that the diameter corrections are larger than those derived by us, as shown in Figure 3 and Figure 7.

As a means of understanding the larger corrections determined by Hering and McMurry (1991), a similar, albeit theoretical, approach was used to compare the theoretical response of PSL ( $m=1.588-0i$ ) to the theoretical response for different indices of refraction. Using the theoretical response corresponding to a specific PSL particle diameter, a corrected diameter for the same value of theoretical response, but for different

refractive index was determined. This method removes the dependence on the normalization constant and on the manufacturer calibration, which as seen in Figure 5 does not resemble a good fit to Mie theory in certain size regions, and is completely theoretical. The multivalued problem arises in this method in the ranges of flat theoretical response.

The ratio of PSL to corrected diameter is shown in Figure 8b for  $m=1.399-2.22 \times 10^{-3}i$  ( $RH=90\%$ ) and  $m=1.530-6.60 \times 10^{-3}i$  ( $RH=0\%$ ). The derived diameter corrections were larger than those of Hering and McMurry (1991) (Figure 8a) for  $m=1.399-2.22 \times 10^{-3}i$  and smaller for  $m=1.530-6.60 \times 10^{-3}i$ . This discrepancy may be caused by the measured atmospheric aerosol having similar response to that of oleic acid ( $m=1.46-0i$ ) as observed by Hering and McMurry, (1991). The scatter occurring at 0.6-0.7  $\mu\text{m}$  is related to the multivalued sections of the Mie curves, and suggests that in these regions, any resolution provided by the probe is artificial; channels in this region should be lumped.

An ideal method for determining diameter corrections relies on the instrument response (an obvious experimental necessity), as well as provides the opportunity for evaluating the multivalued regions of the Mie curve. Although the Mie-Mie method fulfills the second requirement, it is completely theoretical and does not accurately describe the response of the ASASP-X. In the following section an adaptation of the previous methods which meets the stated criteria is described and employed in the correction of data.

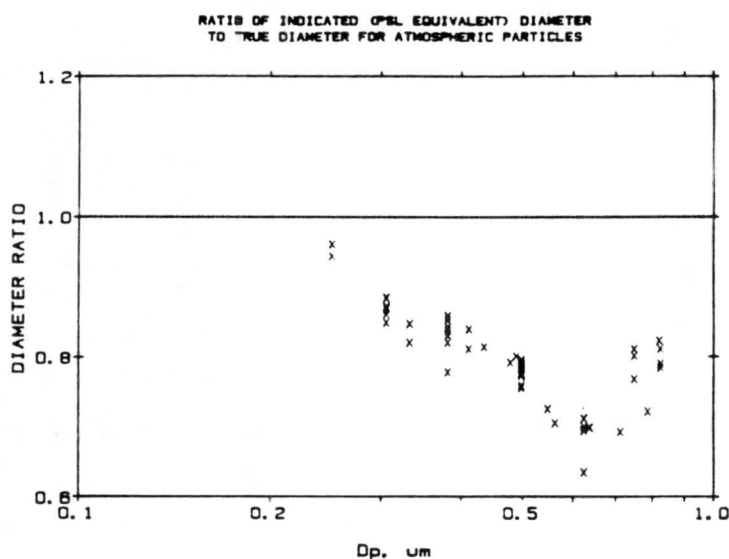


**Figure 8a.** Ratio of PSL to the geometric diameter for atmospheric particles as a function of geometric diameter. (Hering and McMurry, 1991).

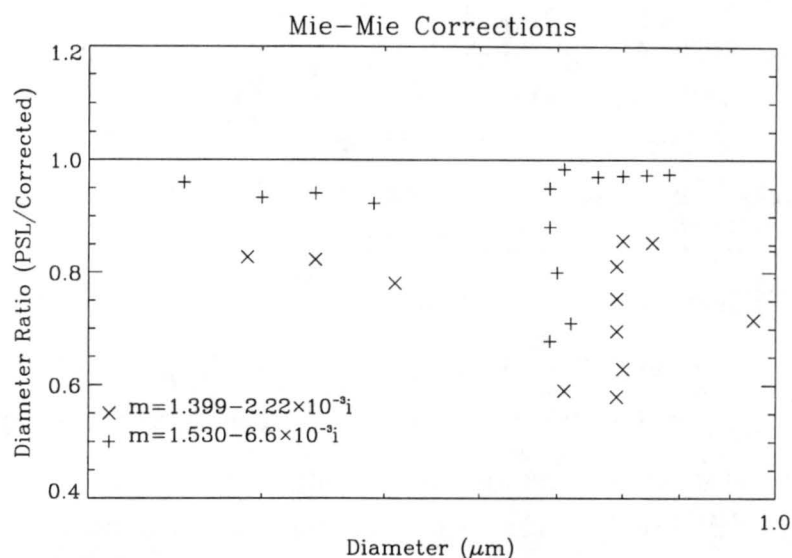


**Figure 8b.** Ratio of PSL to corrected diameter as a function of corrected diameter for Mie-Mie corrections (RH=90% and 0%).

## VI. Polynomial to Mie Curve Corrections

The procedure described here combines techniques from the previous two sections. Using the manufacturer calibration maintains consistency with the ASASP-X probe settings, while comparison with Mie curves eliminates the artificial smoothing through the multivalued sections of the theoretical response introduced by the polynomial-polynomial method (Section IV). By using the normalization constant, the manufacturer voltage calibration can be converted to the theoretical response for a particle of a given refractive index. Similar to previous methods, for a manufacturer calibration cross section corresponding to a PMS diameter, one can determine the corrected diameter corresponding to the same theoretical response value for a Mie curve for a given refractive index.

The primary variable in this method is the normalization constant. Garvey and Pinnick (1983) determined a value of  $C=1.9 \times 10^8 \text{ V cm}^{-2}$  by using experimentally derived response voltages for PSL particles and relating the volts to theoretical response ( $\text{cm}^2$ ). Errors associated with this method can range anywhere from one to five size channels (Garvey and Pinnick, 1983). Different probes may have different normalization constants, and to determine the appropriate constant for our ASASP-X, PSL at one diameter (0.87  $\mu\text{m}$ ) in Range 0 was measured. Using our probe, the size channel corresponding to the peak counts was determined for this size PSL particle. Interpolation between discriminator level voltages for the peak channel was then performed to determine the corresponding voltage for a PSL diameter of 0.87  $\mu\text{m}$ . Fitting this data point to the theoretical response

resulted in a normalization constant of  $C=1.89 \times 10^8 \text{ V cm}^{-2}$ , which applies to all ranges. Figure 9 shows the ratio of PMS to corrected diameters for a normalization constant  $C=1.9 \times 10^8 \text{ V cm}^{-2}$ . Note that the relative gain ratios supplied by Garvey and Pinnick (1983) for other ranges with respect to Range 0 were assumed in constructing this figure.

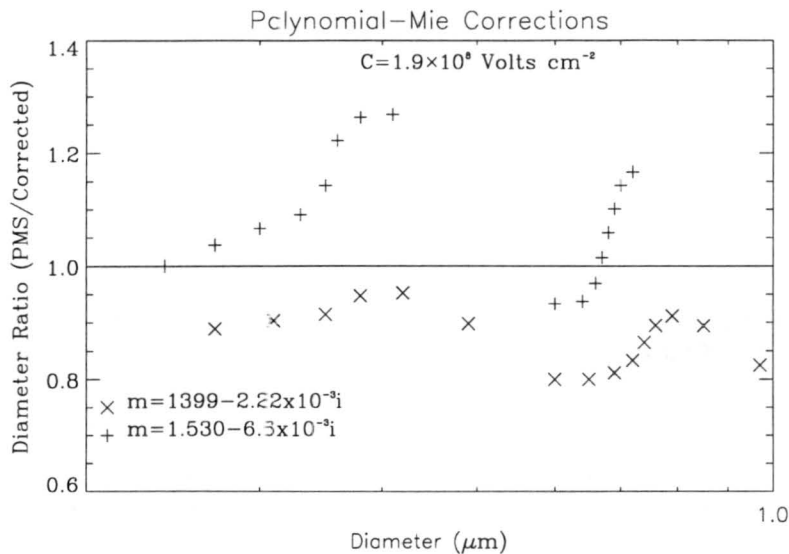


**Figure 9.** Ratio of PMS to corrected diameters as a function of corrected diameters for polynomial-Mie corrections (RH=90% and 0%). A normalization constant of  $C=1.9 \times 10^8 \text{ V cm}^{-2}$  was applied.

To demonstrate the dependence of the corrections on the normalization constant, another value was determined by fitting the manufacturer calibration polynomial to the PSL Mie curve at the diameter of  $0.48 \mu\text{m}$ , which results in a normalization constant of  $C=1.44 \times 10^8 \text{ V cm}^{-2}$ . Figure 10 shows the ratio of PMS to corrected diameters for this normalization constant; using this constant results in much larger corrected diameters for both indices of refraction. The ratios for this method are noticeably different than those for the Mie-Mie method in that ratios greater than 1 are obtained (see Figure 8b).

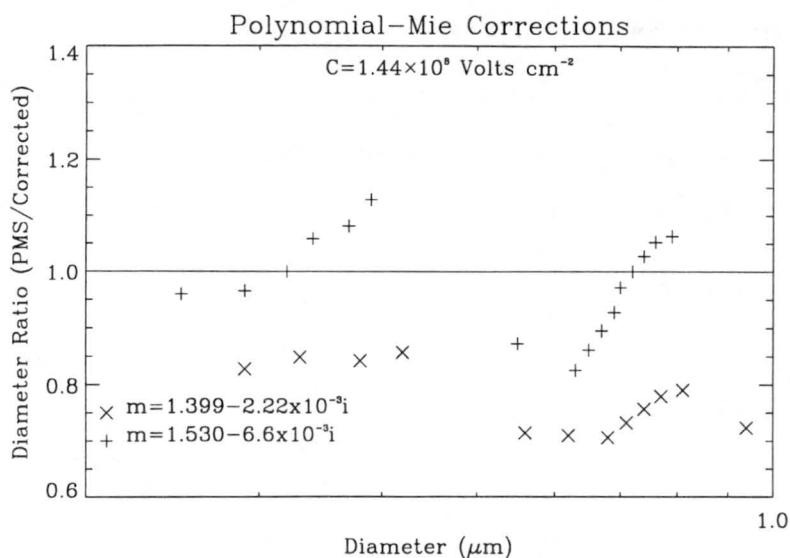


**Figure 10.** Ratio of PMS to corrected diameters as a function of corrected diameters for polynomial-Mie corrections (RH=90% and 0%). A normalization constant of  $C=1.44 \times 10^8 \text{ V cm}^{-2}$  was applied.

**Table 3.** Corrected diameters derived using the polynomial-Mie method for RH=90% and 0%. PMS diameters and corresponding channels are given for comparison. Cross-sections are calculated using the voltages measured for our ASASP-X, with the relative gains in Garvey and Pinnick (1983), and a normalization constant of  $C=1.9 \times 10^8 \text{ V cm}^{-2}$  applied. They differ slightly from the PMS values listed in Table 1.

Bin	PMS Dp ( $\mu\text{m}$ )	Measured Cross Section ( $\text{cm}^2$ )	Cross Section RH=0% ( $\text{cm}^2$ )	Dp RH=0% ( $\mu\text{m}$ )	Cross Section RH=90% ( $\text{cm}^2$ )	Dp RH=90% ( $\mu\text{m}$ )
1	0.24	$3.392 \times 10^{-10}$	$3.392-3.678 \times 10^{-10}$	0.24	$3.392-4.189 \times 10^{-10}$	0.27
2	0.28	$6.143 \times 10^{-10}$	$5.339-6.303 \times 10^{-10}$	0.27	$5.519-6.246 \times 10^{-10}$	0.31
3	0.32	$9.379 \times 10^{-10}$	$8.509-9.772 \times 10^{-10}$	0.30	$8.703-9.631 \times 10^{-10}$	0.35
4	0.36	$1.304 \times 10^{-9}$	$1.273-1.450 \times 10^{-9}$	0.33	$1.282-1.400 \times 10^{-9}$	0.38
5	0.40	$1.716 \times 10^{-9}$	$1.649-1.873 \times 10^{-9}$	0.35	$1.642-1.758 \times 10^{-9}$	0.42
6	0.44	$2.173 \times 10^{-9}$	$2.118-2.376 \times 10^{-9}$	0.36	$2.171-2.183 \times 10^{-9}$	0.49
7	0.48	$2.690 \times 10^{-9}$	$2.636-2.885 \times 10^{-9}$	0.38	$2.643-2.758 \times 10^{-9}$	0.60
8	0.52	$3.252 \times 10^{-9}$	$3.108-3.296 \times 10^{-9}$	0.41	$3.217-3.342 \times 10^{-9}$	0.65
9	0.56	$3.853 \times 10^{-9}$	$3.827-3.907 \times 10^{-9}$	0.60	$3.815-4.019 \times 10^{-9}$	0.69
10	0.60	$4.460 \times 10^{-9}$	$4.216-4.474 \times 10^{-9}$	0.64	$4.248-4.499 \times 10^{-9}$	0.72
11	0.64	$5.085 \times 10^{-9}$	$4.816-5.246 \times 10^{-9}$	0.66	$5.051-5.334 \times 10^{-9}$	0.74
12	0.68	$5.720 \times 10^{-9}$	$5.246-5.760 \times 10^{-9}$	0.67	$5.610-5.871 \times 10^{-9}$	0.76
14	0.72	$6.371 \times 10^{-9}$	$6.334-6.933 \times 10^{-9}$	0.68	$6.326-6.513 \times 10^{-9}$	0.79
14	0.76	$7.025 \times 10^{-9}$	$6.933-7.514 \times 10^{-9}$	0.69	$6.988-7.046 \times 10^{-9}$	0.85
15	0.80	$7.676 \times 10^{-9}$	$7.514-8.049 \times 10^{-9}$	0.70	$7.655-7.691 \times 10^{-9}$	0.97
	0.84	$8.332 \times 10^{-9}$	$8.049-8.526 \times 10^{-9}$	0.72	$8.316-8.602 \times 10^{-9}$	1.04

The polynomial-Mie method automatically groups channels in the regions of flat theoretical response, which is an advantage of using this method. For each refractive index, the multivalued range of the Mie curve is taken into account by this 'natural' lumping. The effects can be seen in Table 3, which gives the corrected diameter and the theoretical response for range 1 for both relative humidities. Notice for RH=0% that channel 8, which in the PMS calibration is bounded by diameters of 0.52 and 0.56  $\mu\text{m}$ , has been corrected to a larger bin bounded by diameters of 0.41 and 0.60  $\mu\text{m}$ . Figure 2 shows that this corrected bin spans the flat region of the Mie theoretical response for that refractive index.

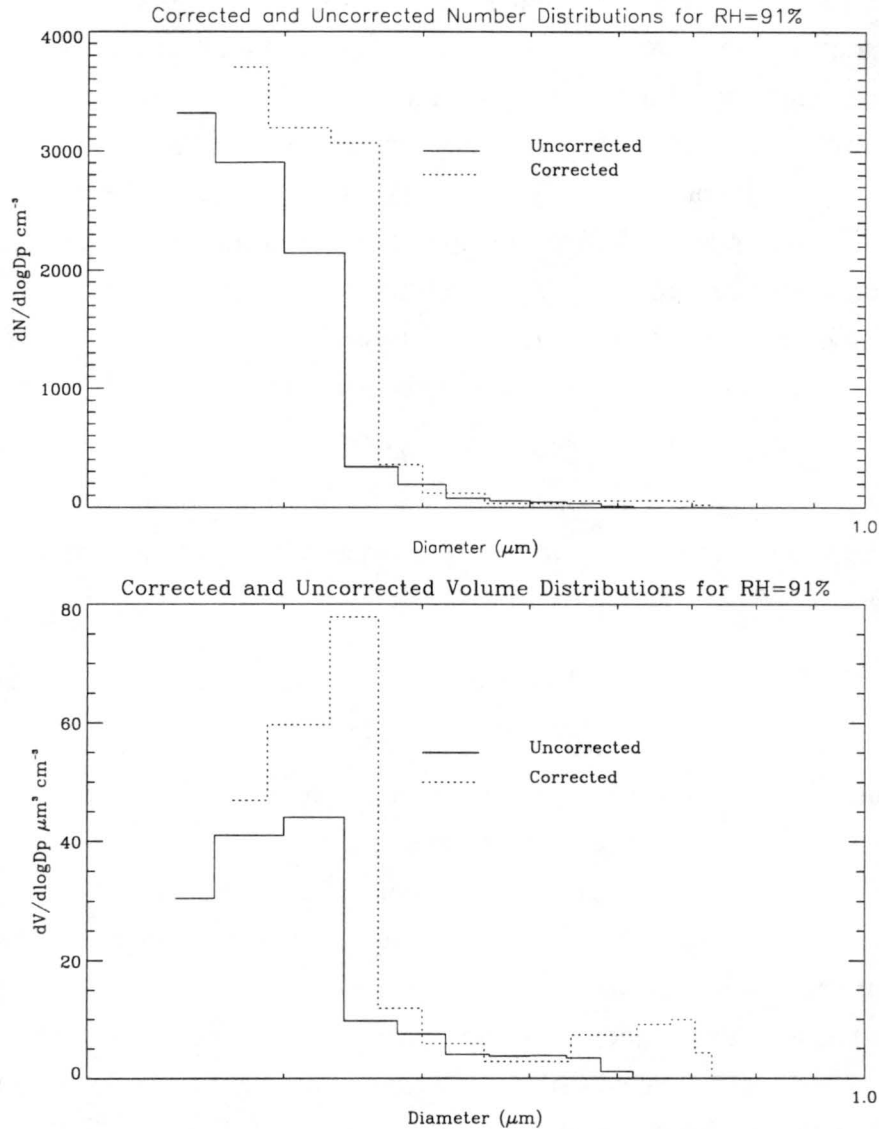
Any variation in the relative gain ratios would also alter the corrected size results. The relative gain ratios provided by Garvey and Pinnick (1983) were used here. Measured discriminator level voltages agreed well with those presented in the PMS manual, and with those from Garvey and Pinnick (1983), however there could be some differences in the relative gains between ranges. Different relative gains would change the curvature of the manufacturer calibration, thereby changing the relationship between it and other Mie curves, resulting in different size corrections. One possible effect of this can be seen by the fact that although only one normalization constant is used for all ranges, we observed that different constants were better fits in certain ranges (e.g.,  $C=1.44 \times 10^8 \text{ V cm}^{-2}$  fit range 1, but was not the best fit in other ranges). For the most accurate results using the polynomial-Mie correction method on data, the relative gain ratios for a particular probe should be measured.

## VII. Applying Diameter Corrections to Data

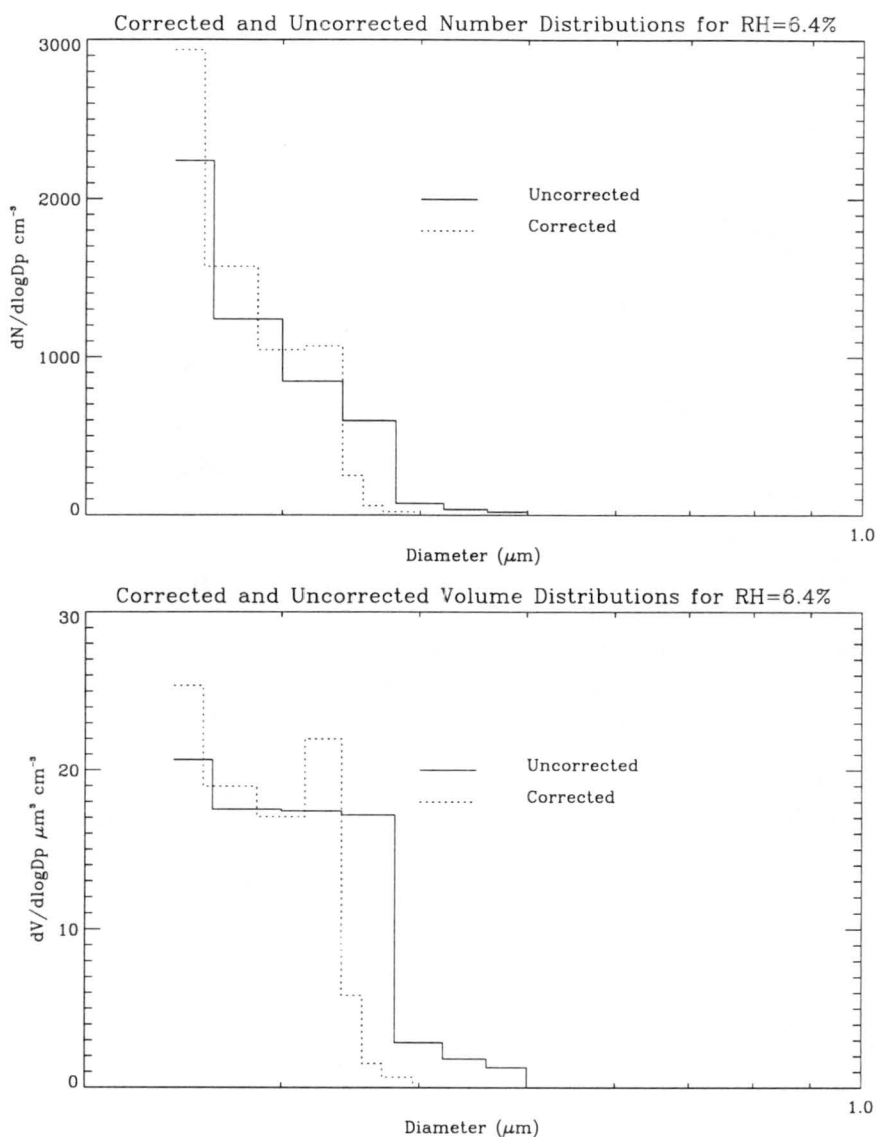
Using data taken 12 August 1995 in the Great Smoky Mountains, diameter corrections determined in Section VI were applied, and number and volume distributions were calculated (Figures 11 and 12). The data correspond to atmospheric aerosols measured at RH=91% and 6.4% with a time difference of 2 hours between the samples. Corrected diameters used to calculate distributions were for indices of refraction from Table 1 for relative humidities of 90% and 0%, respectively.

Figure 11 shows the number and volume distributions for range 1 corresponding to aerosol at RH=91%. Uncorrected distributions were calculated using the PMS diameters. The integrated area under the number distribution are the same for corrected and uncorrected diameters, but the integrated area under the corrected volume distribution is larger by 25%. Because the volume distribution depends on the cube of the diameter, the peak of the corrected distribution shifts to larger size because the corrected diameters are larger than the PMS diameters for RH=90% (see Figure 9).

The distributions in Figure 12 are for aerosol of RH=6.4%. The integrated area under the number distribution is the same for the corrected and uncorrected diameter. For this relative humidity, however, the integrated area for the corrected volume distribution is smaller by 17%. The shift in the corrected distribution is toward smaller sizes because the corrected diameters are smaller than PMS diameters in some size regions for RH=0% (see Figure 9).



**Figure 11.** Corrected and uncorrected number and volume distributions for RH=91%. Corrected diameters were derived using the polynomial-Mie corrected diameters.



**Figure 12.** Corrected and uncorrected number and volume distributions for RH=6.4%. Corrected diameters were derived using the polynomial-Mie corrected diameters.

### Conclusion

Several methods used to determine corrected diameters for the ASASP-X have been investigated in this work. The polynomial-Mie method includes the dependence on the instrument response, and a method for correcting over the multivalued regions of cross section, both of which are required for accurate size determinations. This method was therefore used to derive corrected diameters for the ASASP-X for a range of refractive index. Corrections to data showed significant under or oversizing of volume distributions in comparison to uncorrected data, depending on the refractive index (relative humidity) of the aerosol measured.

## **Acknowledgements**

This work was supported by the National Park Service under Grant No. 1443-CA0001-92-006 96.5.

## **References**

- Active Scattering Aerosol Spectrometer Probe PMS Model ASASP-X Operating Manual. Serial No. 805-0978-10 (1977)
- Bohren, C.F, and Huffman, D.R. (1983). Absorption and Scattering of Light by Small Particles. John Wiley and Sons, New York.
- Hering, S.V., and McMurry P.H., (1991). Optical counter response to monodisperse atmospheric aerosols. *Atmospheric Environment* **25A(2)**:463-468.
- Kim, Y.J., and Boatman, J.F., (1990). Size Calibration Corrections for the Active Scattering Aerosol Spectrometer Probe (ASASP-100X). *Aerosol Science and Technology* **12**:665-672.
- Garvey, D.M., and Pinnick, R.G., (1983) Response Characteristics of the Particle Measuring Systems Active Scattering Aerosol Spectrometer Probe (ASASP-X). *Aerosol Science and Technology* **2**:477-488.